Electrophysiological changes in the acute phase after deep brain stimulation surgery

Lucia K. Feldmann [a], Diogo Coutinho Soriano [b,c], Jeroen Habets [a], Valentina D'Onofrio [d], Jonathan Kaplan [a], Varvara Mathiopoulou [a], Katharina Faust [j], Gerd-Helge Schneider [e], Doreen Gruber [f], Georg Ebersbach [f], Hayriye Cagnan [c], Andrea A. Kühn [a,g,h,i,*]

[a] Movement Disorder and Neuromodulation Unit, Department of Neurology, Charité - Universitätsmedizin Berlin, Charitéplatz 1, 10117, Berlin, Germany
[b] Center of Engineering, Modeling and Applied Social Sciences, Federal Universtiy of ABC, 09606-045, Sao Bernardo do Campo, Brazil
[c] Department of Bioengineering, Imperial College London, London, SW7 2AZ, United Kingdom
[d] Padova Neuroscience Center (PNC), University of Padova, 35131, Padua, Italy
[e] Department of Neurosurgery, Charité - Universitätsmedizin Berlin, Charitéplatz 1, 10117, Berlin, Germany
[f] Movement Disorders Hospital, Kliniken Beelitz GmbH, Strasse nach Fichtenwalde 16, 14547, Beelitz-Heilstätten, Germany
[g] Berlin School of Mind and Brain, Charité University Medicine, Berlin, Germany
[h] NeuroCure Clinical Research Centre, Charité University Medicine, Berlin, Germany
[i] DZNE, German Center for Degenerative Diseases, Berlin, Germany
[j] Department of Neurosurgery, Medical Faculty and University Hospital Düsseldorf, Heinrich-Heine-Universität Düsseldorf, Düsseldorf, Germany

A B S T R A C T

Background: With the introduction of sensing-enabled deep brain stimulation devices, characterization of long-term biomarker dynamics is of growing importance for treatment optimization. The microlesion effect is a well-known phenomenon of transient clinical improvement in the acute post-operative phase. While beta band activity is confirmed as a reliable biomarker for bradykinesia using chronic recordings, little is known about the ideal time point for initial electrophysiology-based programming.

Objective: To investigate the microlesion effect impact in chronic biomarker recordings.

Methods: Subthalamic peak biomarker power was continuously recorded during the first 40 post-operative days in 12 Parkinson's disease patients implanted with a sensing-enabled neurostimulator. Daily change in mean peak power and complexity was analyzed. Additionally, power spectral density at rest was compared between immediate postoperative period and three-months-follow-up. We additionally present continuous pallidal recordings in 2 dystonia patients.

Results: Mean peak power increased postoperatively, and the rate of change stabilized at 22–29 days. Peak power complexity showed a decrease in the number of recurrence states and laminarity, stabilizing around the same time point. Biomarker activity showed a significant increase at 3-month-follow up compared to the early post-operative phase. The microlesion effect was clinically reflected as a decrease in pre-vs. postoperative medication before setting of chronic stimulation parameters.

Conclusions: The transient postoperative microlesional effect is characterized by reduced beta band power and reduced neural signal complexity that gradually stabilize towards the end of the first month after surgery and most likely reflect local neuronal adaptation. These findings are important for the timing of electrophysiology-supported DBS programming, such as contact selection or adaptive algorithms.

1. Introduction

Deep brain stimulation (DBS) is an effective therapy for movement disorders [1–3]. Recordings from DBS electrodes have significantly improved our understanding of electrophysiological changes underlying symptom severity and therapy response. In Parkinson's disease (PD), increased subthalamic activity in the beta frequency band (13–35 Hz) has been identified as a biomarker for bradykinesia [4–9], while in dystonia, lower-frequency activity in the theta band (5–8 Hz) has been identified as a biomarker [10,11]. This information can be used to inform adaptive algorithms [12–14]. However, most of this research has been conducted intra-operatively or during a short peri-operative time window when electrodes are externalized and electrophysiological signals might be affected by the post-operative microlesion effect [4,6,12, 13,15–19]. This microlesion effect leads to a temporary alleviation of clinical symptoms, and can even cause symptoms that usually are

related to overstimulation such as dyskinesia or (hypo)manic episodes in PD patients [20,21] in the absence of stimulation [22]. Microlesion effect induced symptom improvement positively correlated with later DBS effectivity in PD [23]. Electrophysiological patterns during this time period are less well explored. Already during electrode insertion, an immediate beta band activity decrease was observed in intraoperative local field potential (LFP) [24], which aligns with an observed individual increase of beta band activity three months postoperatively compared to immediate post-operative recordings, although the latter did not reach significance on the group level [25].

To date, little is known about the time-course of "recovery" of the electrophysiological activity after electrode insertion. A recent study showed increased periodic activity and decreases in aperiodic components after one month compared to acutely post-operatively [26]. With the growing availability of sensing-enabled neurostimulators, long-term biomarker changes and patterns can be assessed [25,27–31], such as circadian rhythms [32]. Before implementing biomarkers as feedback signals in clinical routine, their temporal reliability to reflect disease-specific symptoms and the stability over time are important prerequisites. Specifically, for adaptive algorithms it becomes important to pin-point when relevant biomarkers, which could be used to control stimulation delivered to the target brain regions, reach a steady-state. In the present study, we aim to characterize the microlesion effect and its temporal dynamics using the chronic brain-sense technology in order to inform future sensing-supported DBS applications, such as adaptive DBS, and contact selection.

2. Material and methods

2.1. Participants

12 PD patients were included in this study. Written informed consent was obtained and the study was conducted in accordance with the ethical standards set by the declaration of Helsinki. The study was approved by the local ethics committees of the Charité Universitätsmedizin Berlin (EA2/256/60, EA1/164/23) and Landesärztekammer Brandenburg (2022-201-BO). After subthalamic DBS implantation [33] with the Percept PC/RC neurostimulator system (Medtronic, Minneapolis, MN, USA), participants were treated in a specialized PD hospital. Inclusion criterion was the complete recording of chronic biomarker data in sensing-enabled DBS-settings during the time of at least 7 days between the post-operative release until re-admission. There were 7 male and 5 female participants at a mean age of 62.3 ± 5.7 years. For more clinical details, see Table 1A. Additionally, two patients with cervical dystonia (1 female, 1 male), implanted with

DBS electrodes in the internal pallidal globe (GPi), were included.

2.2. Data acquisition

The chronic sensing settings are presented in Table 1B, following the procedure as previously described [32]. Individual biomarker peaks were selected in a range between 8 and 25 Hz (mean: 15.9 ± 5.3 Hz). For all participants, LFP data for the initial set-up of sensing, including peak selection, was available for artifact screening. Chronic subthalamic oscillatory activity was assessed using 10 min averages of mean peak-power at a 5 Hz-window around an investigator-selected biomarker peak in the BrainSense mode (see Table 1B) for 12 patients during the post-operative phase of at least 7 days duration. The mean recording duration was 16 ± 10.97 days (mean ± std; recording range: 7–41 days) ranging between 7 and 61 days post-operatively, and analysis was restricted to the first 40 postoperative days, to capture the highest data availability.

For a subset of six patients (Table 1B, Fig. 3), LFP data were assessed through post-operative LFP recordings (subject 6,7,9,10,11,12) and recordings at 3-months-follow-up in the OFF-medication/OFF-stimulation state (at least 12 h withdrawal of dopaminergic medication, switching-off of stimulation at least 30 min before recording). For these patients, also the UPDRS-III-score at both time-points was available (Table 1B, Fig. 3).

All chronic LFP recordings were performed under usual medication that was adjusted 2–3 days after DBS surgery according to clinical symptom improvement and after initialization of DBS. Between pre-operative admission and post-operative hospital release, the mean reduction of dopaminergic therapy (levodopa-equivalent dose, LEDD, calculated according with [34]) was 33 ± 23.8 % (±SD). This serves as a clinical correlate of the post-operative microlesion effect, and our recording period begins after release from the hospital and this medication adjustment. While exact medication schedules were not available, readmission LEDD at the rehabilitation showed only minor changes of LEDD (LEDD post-OP/rehabilitation admission 1.1 ± 16.5 % (±SD). For the patients with dystonia, there was no relevant medication, and DBS was not activated during the recording period.

2.3. Data analysis

All analysis were conducted using Matlab (The Mathworks, Natick, MA, USA), leveraging custom-written toolboxes, which are openly available through github (CircaDiem Toolbox [32], Perceive toolbox [35] and SPM12: https://github.com/spm/spm12). After correction to the central European time-zone, chronic BrainSense data were

Table 1A
Demographic information for study subjects.

SubID	Sex	Age [y]	LEDD pre-OP	LEDD post-OP	LEDD admission rehab	Range DBS [mA] LEFT	Range DBS [mA] RIGHT	UPDRS OFF/OFF post-OP	UPDRS OFF/OFF 3-MFU
sub01	f	60	1025	1025	1025	0.7–0.8	NA	NA	NA
sub02	m	65	1000	300	300	0.5	0.5	21	39
sub03	m	55	900	475	500	1.0–1.1	1.0–1.1	7	28
sub04	f	70	1635	682	782	0.5	0.5	NA	NA
sub05	f	71	1387	1087	NA	1.0–1.1	1.0–1.1	NA	NA
sub06	f	64	773	351	252	0.5–1.0	0.5–1	21	41
sub07	m	55	1035	825	925	0.9–1.8	1.0–1.7	31	43
sub08	m	65	625	625	575	NA	1.0–1.2	NA	NA
sub09	f	53	1232,5	850	1112.5	0.4–0.5	0.4–0.5	49	51
sub10	m	61	1156	724	624	0.5–1	0.5–1	21	36
sub11	m	65	850	375	375	0.5	0.5	39	43
sub12	m	64	575	575	575	2.8–3.2	2.1–2.1	57	54
DYT01	m	55	NA	NA	NA	0	0	NA	NA
DYT02	f	65	NA	NA	NA	0	0	NA	NA

Sex: f=female; m=male; Age: y=years; LEDD= Levodopa-equivalent daily dose at admission for DBS implantation (pre-OP) and release from hospital (post-OP); OP=surgery; rehab=rehabilitation; DBS= deep brain stimulation; UPDRS=Unified Parkinson's Disease Rating Scale; MFU=months-follow-up; NA= not applicable.

Table 1B
Recording information for study subjects.

SubID	start post-OP [days]	end post-OP [days]	Rec. duration [days]	Day for norm.	Cont. LEFT	Cont. RIGHT	ECG artifact RIGHT	ECG artifact LEFT	Peak L [Hz]	Peak R [Hz]
sub01	11	25	14	20	0–2	0–2	yes	no	NA	16
sub02	10	17	7	NA	0–2	0–2	no	no	13	15
sub03	25	39	14	NA	0–2	0–2	no	no	21	22
sub04	20	61	41	21	0–2	0–2	no	no	8	23
sub05	9	27	18	20	0–2	0–2	no	no	12	13
sub06	32	39	7	NA	0–2	0–2	no	no	19	23
sub07	13	23	10	20	0–2	1–3	no	no	8	18
sub08	11	21	10	20	0–2	0–2	yes	no	NA	19
sub09	9	29	20	20	0–2	0–2	no	no	22	12
sub10	10	44	34	20	1–3	1–3	no	no	14	14
sub11	7	16	9	NA	0–2	0–2	no	no	14	25
sub12	21	29	8	22	0–3	0–2	no	no	8	10
DYT01	3	35	32	20	0–2	0–2	no	no	9	16
DYT02	3	35	32	20	0–2	0–2	no	no	21	9

OP=surgery; NA= not applicable, Rec. = Recording; norm.=normalization; Cont.=bipolar recording contact configuration; ECG=electrocardiogram; L=left; R=right.

individually z-scored after removal of outliers 6 times the standard deviation [32] across the analysis period from post-operative release to readmission. For the main analysis, data from the first 40 post-operative days was used. We screened for electrocardiogram (ECG) artifact contamination based on the initially acquired short resting state LFP recordings using the perceive toolbox ECG-artifact detection algorithm [35]. This resulted in 22/24 hemispheres being included in the main analysis.

For the chronic STN peak beta-power recordings, data was normalized by z-scoring across the whole recording period. Mean peak beta-power was calculated across days (allday-means for the whole 24 h, means for estimated day (07:00–21:00) and night (00:00–07:00 and 21:00–00:00) times).

Since timepoints of recordings were heterogeneous, to increase comparability, we additionally normalized daytime activity to a complete day within a range that was common across all recordings in a range between 10 and 15 days post-surgery in a subset of 8 subjects. The respective day is noted in Table 1B. Peak power is expressed as % of the respective values on the "normalization day".

Across normalization strategies, we applied a polynomial fit to the mean peak-beta power across days and defined the rate of change. Additionally, we performed a Bayesian Changepoint Analysis using the Matlab implementation of the BEAST algorithm [36].

Recurrence quantification analysis (RQA) was used to assess the temporal organization (complexity) of peak-beta power across days. This nonlinear data-driven technique characterizes the evolution of peak-beta power over time, considering the similarity between all pairs of observed samples [37–39]. The first step to perform RQA requires the evaluation of the recurrence plot (RP) [40], i.e., a matrix with binary elements, which summarizes the distance between every pair of states $\mathbf{x}$(i) and $\mathbf{x}$(j) obtained after Takens' embedding. The RP associates a dot (RP(i,j) = 1) whenever $\mathbf{x}$(i) is close to $\mathbf{y}$(j) by a threshold ε, and a white pixel otherwise (RP(i,j) = 0), which can be described by:

$$RP(i,j) = \theta\{\varepsilon - \|\boldsymbol{x}(i) - \boldsymbol{x}(j)\|\} \tag{1}$$

in which $\theta\{\cdot\}$ denotes the Heaviside function, $\|\cdot\|$ denotes the L_∞ norm [27], and the time indexes i and j vary from 1 to N samples. The RP provides a graphical representation of the states' recurrence over time and a "fingerprint" for the generative dynamics underlying the time series. As this dynamics may involve the effect of several interacting variables and (usually) just a single observation is available (e.g., a single LFP recording), the states $\mathbf{x}$(i), with $i = 1, 2, \dots N$, are obtained by "unfolding" the observation through the Takens' embedding technique, introducing additional axes using delayed versions of the observed samples [34]. In this study, both the embedding dimension (d_e) and time delay (τ) in Takens' transformation were estimated using the false

nearest neighbor's algorithm and the first minimal information criterion, respectively ($d_e = 3$ and $\tau = 2$).

The binary patterns observed in the RP are objectively quantified by the recurrence measures, defining the RQA. In this study, we assessed the temporal organization using: 1) laminarity (LAM), which ranges from 0 to 1, and is defined as the percentage of RP points in horizontal segments longer than a minimal length (e.g., 2 points, i.e., in non-isolated states, [27]). Laminarity quantifies the tendency of states' persistency, i.e., how long the samples remain unchanged. A LAM decrease indicates less persistency and higher variability across the observation; 2) the recurrence rate (RR), which ranges from 0 to 1, and is defined as the percentage of repetitions in the recurrence plot considering all comparisons made. A higher RR indicates more regular dynamics in which the recurrence of states often occurs, which not necessarily requires laminar behavior. Details concerning RQA, RP, Taken's embedding can be found in Refs. [37,41].

After z-scoring the peak-beta power for each patient, the RQA was applied for samples within day-time interval (7:00–21:00 h) for each day to capture patients' active periods. After an exploratory analysis, the RP threshold was defined in $\varepsilon = 0.5$, aiming at a suitable dynamic range for RQA metrics across the days, avoiding saturation for capturing the complexity progression [41].

In line with the power analysis, a polynomial curve fitting was employed, adjusting the order based on the first goodness-of-fit maxima, i.e., the one with representative variance explained by the day-time RQA metric across days at the lower polynomial order cost.

Correlation analyses, when mentioned, were performed using Pearson's correlation coefficient (r_p) for normally distributed variables, as determined by the D'Agostino & Pearson test. For non-normally distributed variables, Spearman's correlation coefficient (r_s) was used.

For a subset of six patients, 30sec artifact-free rest recordings in a defined OFF medication and OFF DBS state were available post-operatively and at 3-months-follow-up. All LFP data were pre-processed using a 5th order Butterworth filter with a 1 Hz high-pass and 98 Hz low-pass, as well as a band-stop filter at 48–52 Hz. Time series data was transformed to the time-frequency-domain using Morlet wavelet at 8 cycles and a frequency resolution of 1 Hz. The full spectrum was normalized by the mean beta band power (8–35 Hz) at three months-follow up. For statistical analysis, the mean beta band power was compared between post-operative and three-months follow-up recordings using Monte Carlo paired permutation testing (10.000 permutations). Additionally, in line with the chronic BrainSense power values, for each participant, mean beta-power at a 5 Hz-window centered around the individually selected peak frequency was calculated.

3. Results

3.1. Chronic peak biomarker band power increases during the first post-operative month

Mean STN peak-beta power per day revealed an increase in oscillatory power across patients during the recording period, as highlighted by the individual traces from the 18 hemispheres in Fig. 1 A. The polynomial fit to the average obtained across patients showed a change in slope at 22 days (Fig. 1 B). When considering daytime (07:00–21:00, Fig. 1G) and nighttime (21:00–07:00, Fig. 1H) averages separately, power analysis revealed an increase in oscillatory activity during both day and night time (Fig. 1I), with a stabilization around 19–22 days postoperative.

In the additional subanalysis normalized to a common day (Fig. 1D–E), polynomial fit change was identified at post-operative day 24.

For both normalization strategies, we used Bayesian changepoint detection as an additional measure for trend-change detection (Fig. 1C + F). Here, in both cases, day 29 emerged as the day with the highest probability to be a changepoint (z-score, change point probability (cpPr) = 0.73; common-day-normalization, cpPr = 0.98).

In the two patients with dystonia, for z-scored data post-operative day 26 (Fig. 1K) and for common-day normalized data day 28 (Fig. 1N) were detected as changepoints in the polynomial fit, and day 23 (Fig. 1L, cpPr = 0.79) and day 21 (Fig. 1O, cpPr = 0.5) respectively.

3.2. Signal complexity of biomarker activity during the first post-operative month

To further explore peak-beta power characteristics, RQA was used to investigate its temporal organization. Fig. 2A shows an exemplary change of the peak-beta power time-course during the post-operative period, and the corresponding RP (Fig. 2B) for the whole day cycles (0:00–24:00 h). Differently from the sleep periods, characterized by beta power valleys and dense recurrence structures, day-time (7:00–21:00) intervals present distinct recurrence pattern across days. The initial post-operative interval (gray square) presents day-time periods more populated with recurrences, which decreases in the late phase (magenta square). Day-time recurrence quantification analysis (RQA) reveals an increase in complexity and a gradual decrease in laminarity over the course of several days (Fig. 2C). Interestingly, in Parkinson's disease (PD) patients, the mean day-time laminarity stops declining around the 25th post-operative day (Fig. 2D). For dystonic patients, however, this stabilization occurs earlier, around the 18th post-operative day (Fig. 2F). Day-time laminarity reflects the persistence of similar patterns in behavior, and its reduction indicates an increasing complexity in beta activity over time.

Similarly, the day-time recurrence rate (RR) shows a post-operative decline, with stabilization occurring between the 23rd and 25th days in PD patients (Fig. 2E). In dystonic patients, stabilization happens earlier, around the 18th day (Fig. 2G). Recurrence rate measures the density of samples with similar biomarker levels; a decrease in RR suggests fewer recurrences or a reduction in similar states across day-time samples.

Further analysis revealed significant correlations between the mean laminarity (LAM) and recurrence rate (RR) during the 8th–41st post-operative day interval and the mean day-time biomarker peak for PD patients. Specifically, LAM and RR were negatively correlated with biomarker peak ($r_p = -0.61$, p = 0.0001, and $r_p = -0.69$, p < 0.0001, respectively). Similar findings were observed in dystonic patients within the 3rd–35th day interval, with LAM and RR negatively correlating with biomarker peaks ($r_s = -0.59$, p = 0.0003, and $r_s = -0.54$, p < 0.0013, respectively).
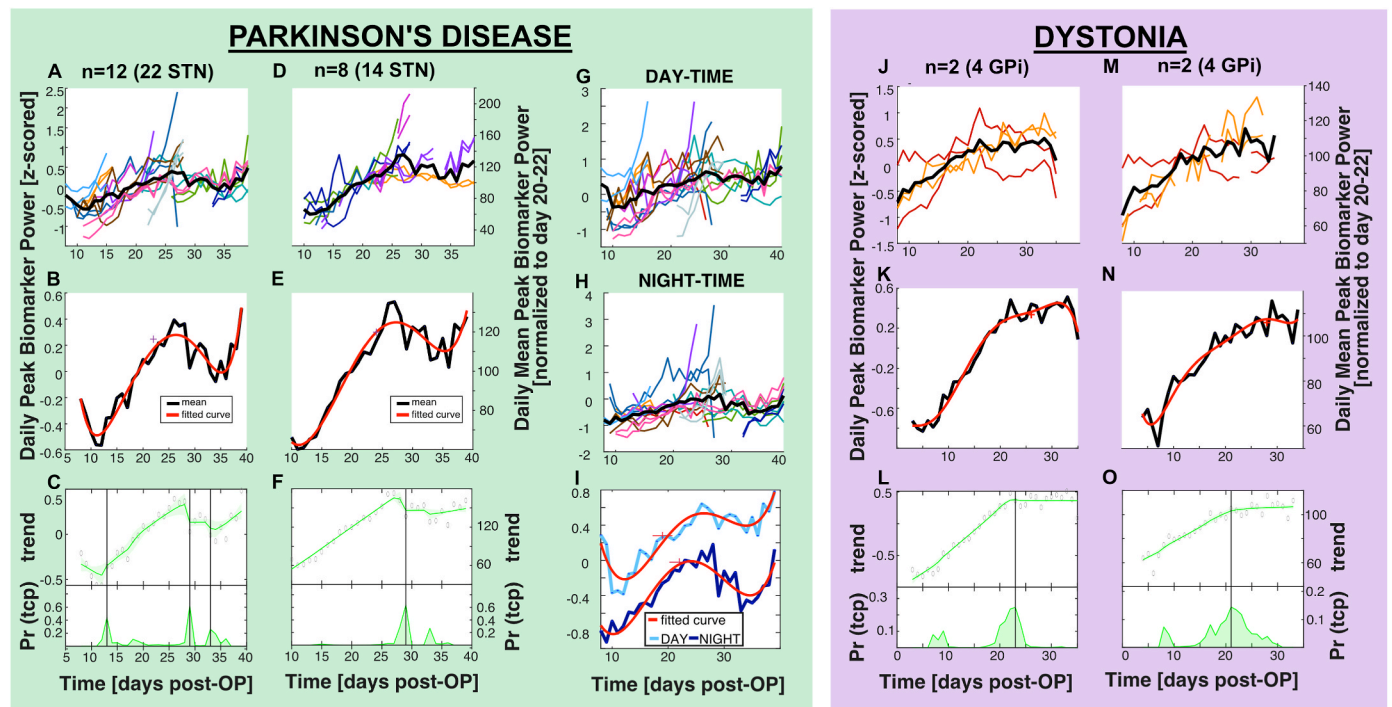

Fig. 1. Biomarker power increases during the first 20 days post-implantation.
Mean z-scored biomarker power per day for each subject individually (colors) and the mean peak activity across subjects in black for the time period 10–40 days post-surgery in patients with PD and subthalamic (STN) DBS **(A)** and dystonia and pallidal (GPi) DBS **(J)**. Biomarker power normalized to common day 20–22 for PD **(D)** and dystonia **(M)**. The polynomial fit reveals a change of slope at 22 days **(B)**, at 24 days **(E)**, and in dystonia at 26 days **(K)** or 28 days **(N)**. Bayesian changepoint detection using the BEAST algorithm [36] **(C,F,L,O)**, displaying the individual trends and Pr (tcp), the posterior probability of a time change point. The overall effect seems to be independent of circadian influences as per the day-time-representation **(G)**, night-time per subject **(H)**, corresponding to panel **(A)**, and the individual fits **(I)**, revealing a change around 20 days, as well.
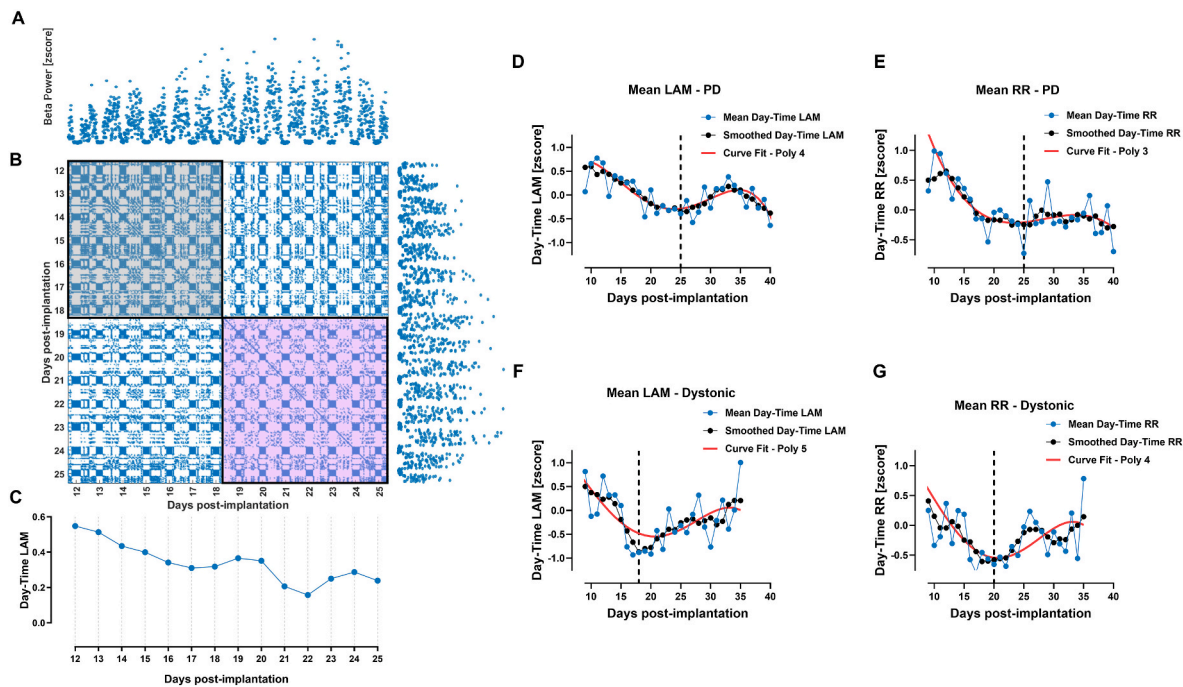
Fig. 2. Recurrence analysis reveals progressive decay of laminarity and recurrence rate during beta recovery after surgery
(A) An exemplary post-implantation beta power (z-scored) time course and its **(B)** recurrence plot illustrating the beta power's proximity for all samples. **(C)** Typical day-time (7:00–21:00 h) laminarity (LAM) decay during the post-implantation period. **(D)** Mean, smoothed (5-points moving average), and curve fitted (4th order polynomial fit) populational day-time LAM (N = 22) for PD patients. **(E)** Mean, smoothed (5-points moving average), and curve fitted (3rd order polynomial fit) populational (N = 22) day-time recurrence rate (RR) for PD patients. **(F)** Mean, smoothed (5-points moving average), and curve fitted (5th order polynomial fit) populational day-time LAM (N = 4) for dystonic patients. **(G)** Mean, smoothed (5-points moving average), and curve fitted (4th order polynomial fit) populational day-time RR (N = 4) for dystonic patients.

3.3. Spectral power in the observed peak frequencies is increased after three months

Beta band activity (13–35 Hz) was smaller in post-operative recordings as compared to 3-months follow-up (Fig. 3 A + C, mean beta band activity normalized to 3-months follow-up: post-operatively: 0.2149 ± 0.097, $p = 0.0003$, n = 12 STN). In analysis centering around the BrainSense selected individual peak-frequency, there was also a significant increase in power at 3-months-follow-up (Fig. 3B, mean normalized peak power, post-operatively: 0.500 ± 0.579, and at 3-months-follow-up: 2.395 ± 1.76, $p = 0.00098$). In line with this, comparison of available post-operative (mean: 30.75 ± 16.6) and 3-months-follow-up UPDRS-III scores (Med OFF, DBS OFF, mean: 41.88 ± 8.2; see Table 1A) showed a significant reduction (paired *t*-test, $p = 0.01$) of motor symptoms during the acute post-operative phase.

4. Discussion

With the availability of chronically sensing-enabled devices, long-term biomarker dynamics can be investigated. Here, we observed that the clinically well-known phenomenon of the post-operative microlesion effect is reflected in electrophysiological biomarker changes. Our data show that together with an increase in beta band power, the complexity of the biomarker signal increases, with a stabilization of beta power and complexity towards the end of the first month (18–29 days) after electrode insertion, regardless of anatomical target structure and underlying pathology.

To date, electrophysiological evidence for the microlesion effect is scarce, with one study investigating the acute intraoperative reduction of beta band activity [24], and one study showing post-operative beta band reduction compared to one month post-surgery [26]. Other studies compared beta band activity after surgery with recordings months to years later [25,42] without showing a microlesion effect, but they did

not evaluate the signal evolution over the immediate postoperative time period.

In our study, daily mean peak power levels rise over time illustrating a potential microlesion effect with the tipping point after 22 days, which is in line with clinically observed changes in motor symptoms and assumed effect of edema. In this cohort, we observed a significant reduction of the immediate post-operative UPDRS motor scores, and a decrease in LEDD already at low DBS intensity in the early post-operative days in comparison with pre-operative LEDD, which supports a clinically relevant microlesion effect. The slow increase in beta band activity over the subsequent weeks in parallel with the clinically known reoccurrence of motor symptoms supports that beta band activity may chronically reflects changes in symptom severity, making it a valid biomarker. Furthermore, our findings point to a stabilization of electrophysiological biomarker only after about 3–4 weeks, which is important to consider for future sensing-based programming, including contact selection and parameter settings for adaptive DBS. Here, reaching a stable state of biomarker activity would be mainly important for thresholding beta band activity for adaptive DBS.

Clinically, there has been a more detailed characterization of the post-OP microlesion effect. Previous studies showed a 35 % improvement of motor performance after DBS lead implantation [22]. In our study, a clear clinical characterization with UPDRS-scores in the same therapeutic condition at beginning and end of the recording period was not available. However, the available OFF-medication/OFF-stimulation UPDRS scores in comparison between 3-months follow up and post-operative OFF Medication/OFF-DBS-states show a significant reduction of motor symptoms post-operatively. Taken together with the knowledge of correlation of increased beta band activity and bradykinetic symptoms [4,6,25,29], the observed biomarker changes point towards a reflection of the microlesion effect. In previous literature, the microlesion effect alone was also related to an improvement of sleep quality, in agreement with improvement of UPDRS scores and scores for
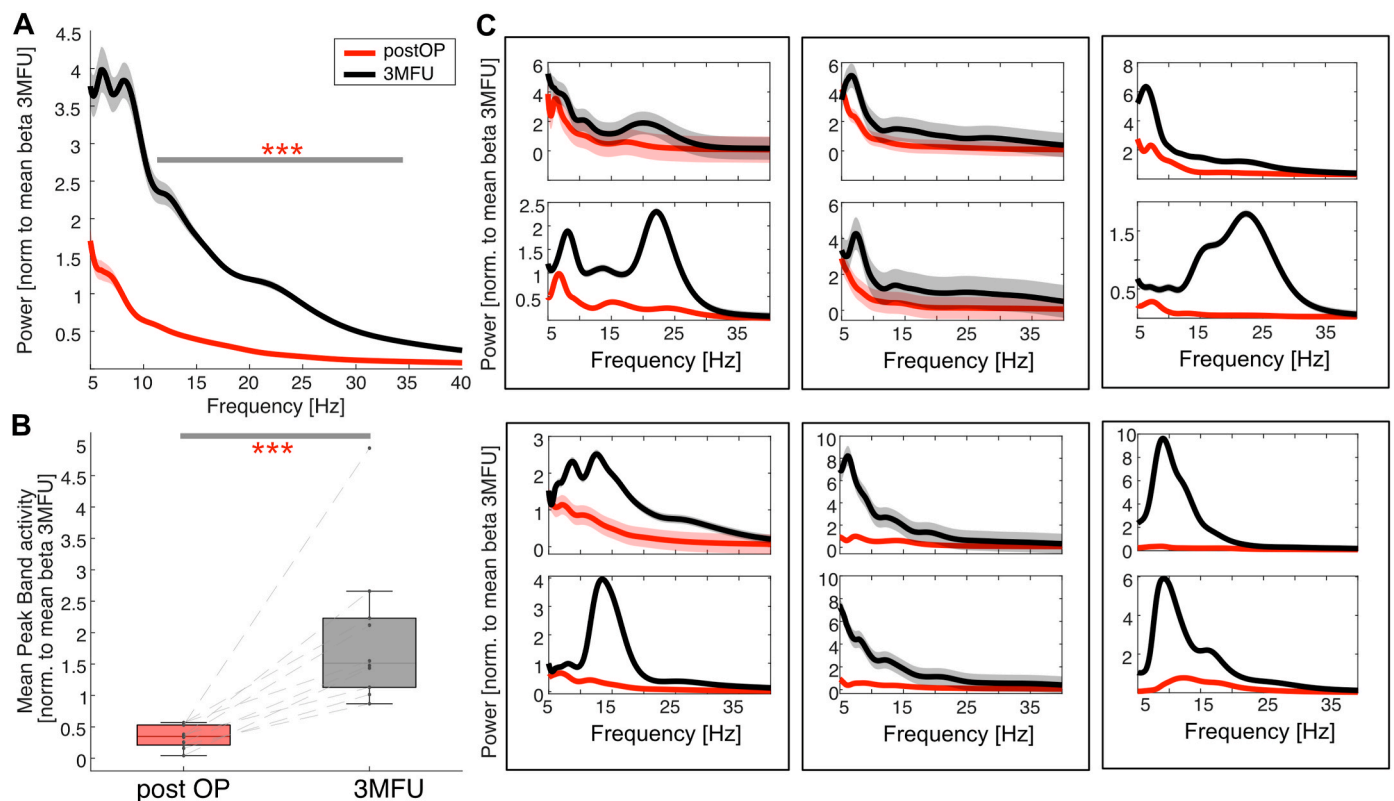
Fig. 3. Post-operative suppression of beta band activity in whole spectral power

(A) Whole-spectrum activity reveals a significant suppression of beta band activity post-operatively, as compared with 3-months-follow-up (Montecarlo paired permutation test, 13–35 Hz, p = 0.0003). **(C)** Representation of individual power spectra post-OP (red) vs. at 3-months-follow-up (black) by hemisphere and subject (box). **(B)** Analysis of the individual spectral power at the selected peak frequency corresponding with the chronic sensing set-up also shows a significant post-operative reduction (p = 0.001).

anxiety and depression, for one month following DBS implantation and before DBS activation [43]. A recovery of the motor symptoms almost to pre-OP baseline values was described for one month [44] up to as much as 6 months [22]. The size of the collateral edema correlated inversely with UPDRS improvement [44].

In line with previous observations of clinical improvements correlating with a wider range of 8–35 Hz [6] and the recent presentation of the clinical utility of aDBS using biomarker also spanning to classical alpha-range peaks [45], we included peaks within the range from 8 to 35 Hz in our study. Another previous concern was that movement artifacts may influence chronically sensed oscillatory activity [32], which may increase during post-operative recovery. Hence, we investigated dynamics separated by day-time and night-time, expecting less influence of movement during the night. In both timespans, we saw a similar pattern of increased biomarker power, suggesting that physiological signal alterations underlie our observations. Moreover, since the electrophysiological microlesion effect is reflected in full-spectral resting-state-activity, we conclude that the changes observed in BrainSense chronic recordings are physiological. Our findings regarding increased beta band activity are in line with a recent study showing increased periodic beta band activity after 1 month compared to acutely post-operatively [26]. Interestingly, this study observed a decrease in aperiodic parameters which might be indicative of increased inhibitory activity.

Other factors influencing electrophysiological recordings at a post-operative phase may relate to the acute post-operative edema, with one study showing a correlation between edema size and left-sided low-beta band activity [46]. [26] reported an additional increase in impedances, as previously observed across DBS targets [47].

Beyond the peak power, we additionally explored the data with

recurrence analysis. Recurrence plots and RQA were first introduced to explore dynamics in non-nonlinear and non-stationary systems [37,48], and have been applied to identify EEG-based markers of autism [33], for seizure detection and localization [34], and for investigating EEG induced patterns during motor cognition [49,50]. In the present study we report a progressive decay in day-time laminarity and recurrence rate, which indicates that the beta rhythm in this interval is *less regular* and exhibits less recurrent states from a dynamical standpoint. The decline in RQA metrics was inversely correlated with the mean beta peak observed across days, suggesting that the stun effect phenomenon underlies the observed trends in beta complexity. Nevertheless, slight alterations in medication and DBS may also contribute to changes in RQA dynamics.

Interestingly, we saw similar dynamics in two first patients with cervical dystonia, continuously recorded in the GPi, who were left OFF-stimulation and did not take relevant neuromodulatory medication. This suggests that increased biomarker activity and signal stabilization after one month may be independent of the underlying pathology, anatomical structure or therapy.

In this study, we used different methods of normalization and changepoint detection. While these approaches yield slightly different results (22–29 days), the general conclusion that can be drawn across conditions and analysis methods is that a change in signal dynamics occurs after the first three post-operative weeks.

Taken together, we would suggest that a reliable set-up for biomarker-based therapies should be conducted after the first post-operative month, to avoid influence on the signal through the microlesion effect. Nevertheless, future adaptive algorithms could also compensate for these changes during the acute post-operative period by employing automated moving baseline adjustment.

Limitations of this study include a small sample size and a lack of clinical characterization during the recording period. Future studies should include more participants to increase external validity, as well as participants from various, e.g. also psychiatric, DBS indications with different target areas to generalize this study's clinical implications. For clinical characterization, additional subjective measures, e.g. patient-reported outcomes, and objective measures, such as sensor-based movement analysis or formalized regular assessments of the UPDRS-III, could be added to correlate with symptomatic changes. In this study, patients received medication and stimulation during the observation period, at a stable and low dose. A reliable tracking of even minor medication adjustments and stratification for this in future analysis may help in identifying medication effects on chronic biomarker dynamics.

5. Conclusion

Here, for the first time, we report a change in the electrophysiological characteristics of chronic biomarker recordings in the acute postoperative state in PD patients treated with subthalamic DBS and two dystonia patients with pallidal DBS. There is both an initial decrease in peak biomarker power and a decreased regularity of complexity measures such as laminarity and the recurrence. These changes may reflect the post-operative microlesion effect, with a transition point towards the end of the first month after DBS surgery. Hence, our data suggest that electrophysiology-based programming of DBS settings or adjustment of adaptive algorithms should be performed after this adaptation phase.

CRediT authorship contribution statement

Lucia K. Feldmann: Writing – original draft, Methodology, Data curation, Visualization, Formal analysis, Conceptualization. **Diogo Coutinho Soriano:** Writing – original draft, Formal analysis, Visualization, Data curation. **Jeroen Habets:** Writing – review & editing, Data curation. **Valentina D'Onofrio:** Writing – review & editing, Formal analysis. **Jonathan Kaplan:** Data curation, Writing – review & editing. **Varvara Mathiopoulou:** Data curation, Writing – review & editing. **Katharina Faust:** Data curation, Writing – review & editing. **Gerd-Helge Schneider:** Data curation, Writing – review & editing. **Doreen Gruber:** Data curation, Writing – review & editing. **Georg Ebersbach:** Data curation, Writing – review & editing. **Hayriye Cagnan:** Data curation, Supervision, Writing – review & editing. **Andrea A. Kühn:** Resources, Funding acquisition, Writing – review & editing, Supervision, Project administration.

Data statement

As individual patient data falls under the health data category of the European General Data Privacy Regulation, a formal data sharing agreement can be set in place upon reasonable request to the corresponding author.

Declaration of competing interest

AAK declares that she is on the advisory board of Medtronic and Boston Scientific, and has received honoraria from Medtronic and Boston Scientific, GHS, LKF received honoraria for talks for Medtronic; no other relationships or activities that could appear to have influenced the submitted work. GE received honoraries for consultancies at AbbVie GmbH, Britannia Ltd., Canopy Medical GmbH, ESTEVE GmbH, Stada GmbH, BIAL GmbH, Desitin GmbH, Neuraxpharm GmbH, Boehringer GmbH and honoraries for lectures at AbbVie GmbH, BIAL GmbH, Cogitando GmbH, Desitin GmbH, ESTEVE GmbH, Licher GmbH, Milupa GmbH, Stada Pharma GmbH, Zambon GmbH, as well as royalties for Kohlhammer Verlag, Springer/Nature-Verlag, Thieme Verlag. DG received speaker honoraria from Ever-Pharma and Abbvie. DCS, VM, JH,VD, KF and HC have nothing to declare.

References

[1] Deuschl G, et al. A randomized trial of deep-brain stimulation for Parkinson's disease. N Engl J Med 2006;355(9):896–908.
[2] Schuurman PR, et al. A comparison of continuous thalamic stimulation and thalamotomy for suppression of severe tremor. N Engl J Med 2000;342(7):461–8.
[3] Vidailhet M, et al. Bilateral deep-brain stimulation of the globus pallidus in primary generalized dystonia. N Engl J Med 2005;352(5):459–67.
[4] Brown P, et al. Dopamine dependency of oscillations between subthalamic nucleus and pallidum in Parkinson's disease. J Neurosci 2001;21(3):1033–8.
[5] Kuhn AA, et al. High-frequency stimulation of the subthalamic nucleus suppresses oscillatory beta activity in patients with Parkinson's disease in parallel with improvement in motor performance. J Neurosci 2008;28(24):6165–73.
[6] Kuhn AA, et al. Reduction in subthalamic 8-35 Hz oscillatory activity correlates with clinical improvement in Parkinson's disease. Eur J Neurosci 2006;23(7):1956–60.
[7] Lofredi R, et al. Beta bursts during continuous movements accompany the velocity decrement in Parkinson's disease patients. Neurobiol Dis 2019;127:462–71.
[8] Tinkhauser G, et al. Beta burst dynamics in Parkinson's disease OFF and ON dopaminergic medication. Brain 2017;140(11):2968–81.
[9] Neumann WJ, Kuhn AA. Subthalamic beta power-Unified Parkinson's disease rating scale III correlations require akinetic symptoms. Mov Disord 2017;32(1):175–6.
[10] Neumann WJ, et al. A localized pallidal physiomarker in cervical dystonia. Ann Neurol 2017;82(6):912–24.
[11] Scheller U, et al. Pallidal low-frequency activity in dystonia after cessation of long-term deep brain stimulation. Mov Disord 2019;34(11):1734–9.
[12] Arlotti M, et al. Eight-hours adaptive deep brain stimulation in patients with Parkinson disease. Neurology 2018;90(11):e971–6.
[13] Little S, et al. Adaptive deep brain stimulation in advanced Parkinson disease. Ann Neurol 2013;74(3):449–57.
[14] Velisar A, et al. Dual threshold neural closed loop deep brain stimulation in Parkinson disease patients. Brain Stimul 2019;12(4):868–76.
[15] Basha D, et al. Beta band oscillations in the motor thalamus are modulated by visuomotor coordination in essential tremor patients. Front Hum Neurosci 2023;17:1082196.
[16] Eisinger RS, et al. Distinct Roles of the human subthalamic nucleus and dorsal pallidum in Parkinson's disease impulsivity. Biol Psychiatry 2022;91(4):370–9.
[17] Hirschmann J, et al. A direct relationship between oscillatory subthalamic nucleus-cortex coupling and rest tremor in Parkinson's disease. Brain 2013;136(Pt 12):3659–70.
[18] Mandali A, et al. Acute time-locked alpha frequency subthalamic stimulation reduces negative emotional bias in Parkinson's disease. Biol Psychiatry Cogn Neurosci Neuroimaging 2021;6(5):568–78.
[19] Tamir I, et al. Eight cylindrical contact lead recordings in the subthalamic region localize beta oscillations source to the dorsal STN. Neurobiol Dis 2020;146:105090.
[20] Gago MF, et al. Transient disabling dyskinesias: a predictor of good outcome in subthalamic nucleus deep brain stimulation in Parkinson's disease. Eur Neurol 2009;61(2):94–9.
[21] Romito LM, et al. Transient mania with hypersexuality after surgery for high frequency stimulation of the subthalamic nucleus in Parkinson's disease. Mov Disord 2002;17(6):1371–4.
[22] Mann JM, et al. Brain penetration effects of microelectrodes and DBS leads in STN or GPi. J Neurol Neurosurg Psychiatry 2009;80(7):794–7.
[23] Lange SF, et al. The intraoperative microlesion effect positively correlates with the short-term clinical effect of deep brain stimulation in Parkinson's disease. Neuromodulation 2023;26(2):459–65.
[24] Chen CC, et al. Intra-operative recordings of local field potentials can help localize the subthalamic nucleus in Parkinson's disease surgery. Exp Neurol 2006;198(1):214–21.

[25] Neumann WJ, et al. Long term correlation of subthalamic beta band activity with motor impairment in patients with Parkinson's disease. Clin Neurophysiol 2017; 128(11):2286–91.

[26] Peng C, et al. Subthalamic nucleus dynamics track microlesion effect in Parkinson's disease. Front Cell Dev Biol 2024;12:1370287.

[27] Kehnemouyi YM, et al. Modulation of beta bursts in subthalamic sensorimotor circuits predicts improvement in bradykinesia. Brain 2021;144(2):473–86.

[28] Steiner LA, et al. Subthalamic beta dynamics mirror Parkinsonian bradykinesia months after neurostimulator implantation. Mov Disord 2017;32(8):1183–90.

[29] Feldmann LK, et al. Toward therapeutic electrophysiology: beta-band suppression as a biomarker in chronic local field potential recordings. npj Parkinson's Dis 2022; 8(1):44.

[30] Alagapan S, et al. Cingulate dynamics track depression recovery with deep brain stimulation. Nature 2023;622(7981):130–8.

[31] Provenza NR, et al. Long-term ecological assessment of intracranial electrophysiology synchronized to behavioral markers in obsessive-compulsive disorder. Nat Med 2021;27(12):2154–64.

[32] van Rheede JJ, et al. Diurnal modulation of subthalamic beta oscillatory power in Parkinson's disease patients during deep brain stimulation. npj Parkinson's Dis 2022;8(1):88.

[33] Feldmann LK, et al. Risk of infection after deep brain stimulation surgery with externalization and local-field potential recordings: twelve-year experience from a single institution. Stereotact Funct Neurosurg 2021;99(6):512–20.

[34] Jost ST, et al. Levodopa dose equivalency in Parkinson's disease: updated systematic review and proposals. Mov Disord 2023;38(7):1236–52.

[35] Neumann WJ, et al. The sensitivity of ECG contamination to surgical implantation site in brain computer interfaces. Brain Stimul 2021;14(5):1301–6.

[36] Zhao KWMA, Hu T, Bright R, Wu Q, Qin H, Li Y, Toman E, Mallick B, Zhang X, Brown M. Detecting change-point, trend, and seasonality in satellite time series data to track abrupt changes and nonlinear dynamics: a Bayesian ensemble algorithm. Remote Sens Environ 2019;232:111181.

[37] Marwan N, et al. Recurrence plots for the analysis of complex systems. Phys Rep 2007;438(5):237–329.

[38] Schinkel S, Marwan N, Kurths J. Order patterns recurrence plots in the analysis of ERP data. Cogn Neurodyn 2007;1(4):317–25.

[39] Webber CL, et al. Simpler methods do it better: success of Recurrence Quantification Analysis as a general purpose data analysis tool. Phys Lett 2009;373 (41):3753–6.

[40] Eckmann J-P, Oliffson Kamphorst S, Ruelle D. Recurrence plots of dynamical systems. Europhys Lett 1987;4(9).

[41] Marwan N. HOW to avoid potential pitfalls in recurrence plot based data analysis. Intl J Bifurc Chaos 2011;21(4):1003–17.

[42] Giannicola G, et al. Subthalamic local field potentials after seven-year deep brain stimulation in Parkinson's disease. Exp Neurol 2012;237(2):312–7.

[43] Ma R, et al. Sleep outcomes and related factors in Parkinson's disease after subthalamic deep brain electrode implantation: a retrospective cohort study. Ther Adv Neurol Disord 2023;16:17562864231161163.

[44] Jech R, et al. The subthalamic microlesion story in Parkinson's disease: electrode insertion-related motor improvement with relative cortico-subcortical hypoactivation in fMRI. PLoS One 2012;7(11):e49056.

[45] Herrington T, et al. Abstract 1219: enrollment phase sensing data from the adaptive DBS algorithm forPersonalized therapy in Parkinson's disease (ADAPT-PD) clinicaltrial, in: abstracts of the 2023 international congress of Parkinson's disease and movement disorders. Mov Disord 2023;38(Suppl 1):S541.

[46] Prenassi M, et al. Peri-lead edema and local field potential correlation in post-surgery subthalamic nucleus deep brain stimulation patients. Front Hum Neurosci 2022;16:950434.

[47] Lungu C, et al. Temporal macrodynamics and microdynamics of the postoperative impedance at the tissue-electrode interface in deep brain stimulation patients. J Neurol Neurosurg Psychiatry 2014;85(7):816–9.

[48] Marwan N. A historical review of recurrence plots. Eur Phys J Spec Top 2008;164 (1):3–12.

[49] Pitsik E, et al. Motor execution reduces EEG signals complexity: recurrence quantification analysis study. Chaos: Interdiscip J Nonlinear Sci 2020;30(2).

[50] Rodrigues PG, et al. Space-time recurrences for functional connectivity evaluation and feature extraction in motor imagery brain-computer interfaces. Med Biol Eng Comput 2019;57(8):1709–25.